COPERNICUS
MARINE ENVIRONMENT MONITORING SERVICE

QUALITY INFORMATION DOCUMENT

Black Sea Waves analysis and forecast product

BLKSEA_ANALYSIS_FORECAST_WAVES_007_003

Issue: 1.2

Contributors: Joanna Staneva, Arno Behrens, Gerhard Gayer, Elisaveta Peneva

Approval date by the CMEMS product quality coordination team:

CHANGE RECORD

When the quality of the products changes, the QuID is updated and a row is added to this table. The third column specifies which sections or sub-sections have been updated. The fourth column should mention the version of the product to which the change applies.

Issue	Date	§	Description of Change	Author	Validated By
1.0	08/01/2018	All	First version of document of CMEMS V4	A. Behrens, J. Staneva, G. Gayer	E. Peneva
1.1	26/03/2018	All	Minor corrections by Mercator after V4 review	F. Hernandez	F. Hernandez
1.2	22/02/2019	All	Adapting the description of the forecasting system from 5 to 10 days forecast release	J. Staneva	

TABLE OF CONTENTS

I EXECUTIVE SUMMARY

I.1 Products covered by this document

This document describes the quality of the analysis and forecast nominal product of the wave component of the Black Sea: BLKSEA_ANALYSIS_FORECAST_WAV_007_003. The product includes the following 2D 1-hourly analysis and forecast instantaneous fields of:

- VHMO: spectral significant wave height (Hm0);
- VTM10: spectral moments (-1,0) wave period (Tm-10);
- VTM02: spectral moments (0,2) wave period (Tm02);
- VTPK: wave period at spectral peak / peak period (Tp);
- VMDR: mean wave direction from (Mdir);
- VPED: wave principal direction at spectral peak;
- VSDX: stokes drift U;
- VSDY: stokes drift V;
- VHM0_WW: spectral significant wind wave height;
- VTM01_WW: spectral moments (0,1) wind wave period;
- VMDR_SW1: mean wind wave direction from;
- VHM0_SW1: spectral significant primary swell wave height;
- VTM01_SW1: spectral moments (0,1) primary swell wave period;
- VMDR_SW1: mean primary swell wave direction from;
- VHM0_SW2: spectral significant secondary swell wave height;
- VTM01_SW2: spectral moments (0,1) secondary swell wave period; and
- VMDR_SW2: mean secondary swell wave direction from

The output data are produced at 1/36°x1/27° horizontal resolution,

I.2 Summary of the results

The quality of the hindcast component of the V4 Black Sea MFC wave product used to produce the BLKSEA_ANALYSIS_FORECAST_WAV_007_003 has been accessed via comparison against satellite observations recorded by the radar altimeters of Sentinel-3a for the time period 06/04/2016 to 20/08/2017 and Jason-3 for the time period 01/12/2015 to 30/09/2017. The horizontal spatial grid resolution of the BS-waves model is 1/27° in zonal direction, 1/36° in meridional direction (ca. 3 km). The assessment of the corresponding wave hindcast is the best way of understanding the validity of the WAM domain model underpinning these products, since the wave analysis-forecast system provided to CMEMS will run without data assimilation and without information from a hydrodynamic model. The growth of errors in the wave forecasts is dominated by growth errors in the forcing fields, which are the U_{10} wind fields from the IFS (Integrated Forecasting System) of the ECMWF.

The main results of the BLKSEA_ANALYSIS_FORECAST_WAV_007_003 quality product assessment are summarized below:

Significant Wave Height: Since the lack of buoy data for the Black Sea, nearly all comparisons for the significant wave heights have been done with satellite altimeter data obtained by the Sentinel-3a and

Jason-3 satellite. The V4 BS-waves system presents good accuracy in terms of the SWH. The model skill enhancement is evident when considering the different statistical parameters and the skills critically depends upon the quality of the wind forcing for the Black Sea. The wave model results and observations are correlated at a level of about 0.9. In general, the wave model tends to underestimate the satellite measurements. The BIAS is always negative with values between 14.2 and 20.7 cm for Jason-3 (better in 2017: 14.2 – 14.5 cm) and 21.3 to 23.6 for Sentinel-3a. That is due to the driving wind fields, which are not only coarse in space but also in time. Using six-hourly wind fields induce an underestimation of the significant wave heights because during such a long time period, wind peaks occurring in between are definitely missed. Furthermore, we assume that the measurements recorded by the radar altimeter of the satellites are systematically too high in general, especially for the Sentinel-3a data.

An important issue for the BS-WAVES Product validation is the lack of systematic in-situ measurements

I.3 Estimated Accuracy Numbers

Estimated Accuracy Numbers (EANs) for the results of the BS-waves system are the mean of the differences between measured and computed values “BIAS” and the corresponding RMS differences. EANs are computed for:

- Significant Wave Height (SWH): refers to the "spectral significant wave height (Hm0)"

The observations are:

- Significant wave height recorded by the radar altimeter of the satellite Sentinel-3a and Jason-3 (that are available on the public server of AVISO (anonymous@avisoftp.cnes.fr))

The EANS computed for the V4 version of the CMEMS Black Sea wave modelling system are based on the simulation of the system in hindcast mode for a two years time period between December 2015 and November 2017. With regard to the lack of systematic in-situ measurements in the Black Sea, satellite measurements are the only continuous source to compare the wave model results with. The final values for BIAS and RMSD are given in Table 1 for each of the four quarters of 2016 and the first three quarters of 2017. Since the BIAS is the difference model mean minus mean of the measurements, the EANs for the BS-waves system indicate an underestimation of the measurements by the wave model, which is mainly due to the coarse resolution of the driving wind fields in time (6-hourly).

***Table 1** : EANs for the current BS-waves system*

	2016 Q1		2016 Q2		2016 Q3		2016 Q4		2017 Q1		2017 Q2		2017 Q3	
	bias	RMSD	bias	RMSD	bias	RMSD	bias	RMSD	bias	RMSD	bias	RMSD	bias	RMSD
Jason-3	-16.7	30.3	-13.2	26.5	-18.4	28.0	-20.7	32.6	-14.2	29.3	-14.5	27.4	-14.3	26.3
Sentinel-3a	no data available								-21.3	34.9	no data		-23,6	33,4
	all values in centimetres													

II PRODUCTION SYSTEM DESCRIPTION

II.1 Production centre details

PU: HZG, Germany

Production chain: BS-MFC-WAVES

External product (2D):

- VHMO: spectral significant wave height (Hm0);
- VTM10: spectral moments (-1,0) wave period (Tm-10);
- VTM02: spectral moments (0,2) wave period (Tm02);
- VTPK: wave period at spectral peak / peak period (Tp);
- VMDR: mean wave direction from (Mdir);
- VPED: wave principal direction at spectral peak;
- VSDX: stokes drift U;
- VSDY: stokes drift V;
- VHM0_WW: spectral significant wind wave height;
- VTM01_WW: spectral moments (0,1) wind wave period;
- VMDR_SW1: mean wind wave direction from;
- VHM0_SW1: spectral significant primary swell wave height;
- VTM01_SW1: spectral moments (0,1) primary swell wave period;
- VMDR_SW1: mean primary swell wave direction from;
- VHM0_SW2: spectral significant secondary swell wave height;
- VTM01_SW2: spectral moments (0,1) secondary swell wave period; and
- VMDR_SW2: mean secondary swell wave direction from

Frequency of model output: hourly (instantaneous)

Geographical coverage : : 27.73°E → 41.96°E ; 40.86°N → 46.80°N (the Azov Sea is excluded)

Horizontal resolution : 1/27° in zonal direction, 1/36° in meridional direction (ca. 3 km)

Vertical coverage: Surface

Length of forecast: 10 days

Frequency of forecast release: Daily

Analyses: No

Hindcast: Yes (one day)

Frequency of hindcast release: Daily

The wave forecasts for the Black Sea are produced by the HZG Production Unit by means of the WAM wave model (described below).
The BS-waves system runs once per day starting at 12:00:00 UTC. It produces 10-day (240 h) forecast fields, initialized by a 1-day (24 h) hindcast.

The BS-waves system integration is composed of several steps:

1. Upstream Data Acquisition, Pre-Processing and Control of: ECMWF (European Centre for Medium-Range Weather Forecasts) NWP (Numerical Weather Prediction) atmospheric forcing.
2. Hindcast/Forecast: WAM produces one day of hindcast and 10 days of forecast.
3. Post processing: the model output is processed in order to obtain the products for the CMEMS catalogue.
4. Output delivery.

The BLKSEA_ANALYSIS_FORECAST_WAV_007_003 production chain is represented in figure 1.

Production Day	FC Cycle	Day	-2	-1	0	1	2	3	4	5	6	7	8	9													
Tuesday	**1**	Tu		H	F	F	F	F	F	F	F	F	F	F													
Wednesday	1	We			H	F	F	F	F	F	F	F	F	F	F												
Thursday	1	Th				H	F	F	F	F	F	F	F	F	F	F											
Friday	1	Fr					H	F	F	F	F	F	F	F	F	F	F										
Saturday	1	Sa						H	F	F	F	F	F	F	F	F	F	F									
Sunday	1	Su							H	F	F	F	F	F	F	F	F	F	F								
Monday	1	Mo								H	F	F	F	F	F	F	F	F	F	F							
Tuesday	**2**	Tu									H	F	F	F	F	F	F	F	F	F	F						
Wednesday	2	We										H	F	F	F	F	F	F	F	F	F	F					
Thursday	2	Th											H	F	F	F	F	F	F	F	F	F	F				
Friday	2	Fr												H	F	F	F	F	F	F	F	F	F	F			
Saturday	2	Sa													H	F	F	F	F	F	F	F	F	F	F		
Sunday	2	Su														H	F	F	F	F	F	F	F	F	F	F	
Monday	2	Mo															H	F	F	F	F	F	F	F	F	F	F

H Hindcast 1 hr

F Forecast 1 hr

Figure 1: *BS-WAV Production Chain*

II.2 System Description

This document details the quality of products from the Black Sea Wave Analysis and Forecast system. These products are generated using a WAM Cycle 4.6.2 3 Black Sea model (spatial resolution about 3 km), which became operational within CMEMS in April 2017. The wave model provides a description of ocean surface gravity wave (periods 1.5 to 25 seconds) characteristics as an extension to the existing physical and ecosystem model products provided by the North-West Shelf MFC. The following subsections describe the model component and its dependencies in terms of models providing the forcing.

Region, grid and bathymetry

The regional wave model for the semi-enclosed Black Sea runs in shallow water mode on a model grid situated between 40°51’36” N to 046°48’16” N and 27°22’12” E to 41°57’45” E, with a spatial resolution of about 3 km, also 100 seconds in latitude, respectively 133 seconds in longitude. The required bathymetry for the model grid bases upon the General Bathymetric Chart of the Oceans (GEBCO, http://www.gebco.net) 1-arc minute data. The bathymetry is only a controlling mechanism on the wave field for depths below approximately 490 m, based on a minimum frequency in the model of approximately 0.04 Hz (period 25 seconds). The model area and the corresponding depth distribution are shown in figure 2.

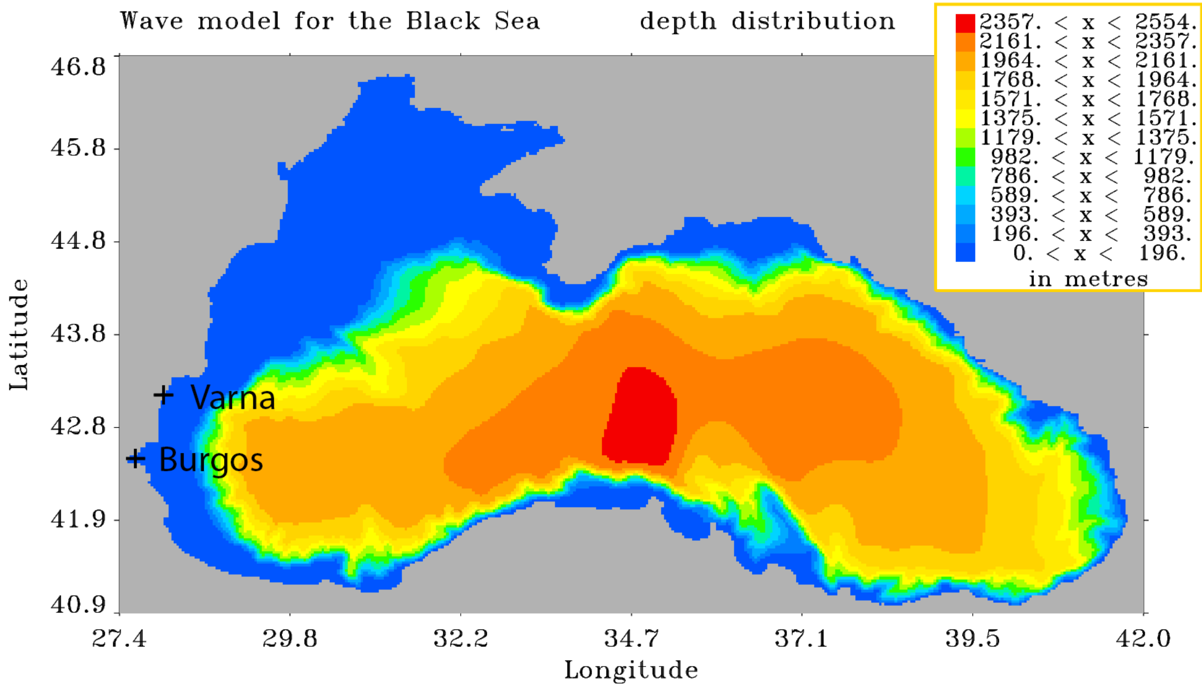

Figure 2 : *Black Sea Wave model WAM depth distribution*

Spectral grid

WAM calculates the two-dimensional energy density spectrum at each of the 44699 active model grid points in the frequency and directional space. The solution of the energy balance equation is provided for 24 directional bands at 15° each, starting at 7.5° and measured clockwise with respect to true north, and 30 frequencies logarithmically spaced from 0.042 Hz to 0.66 Hz at intervals of $\Delta f/f = 0.1$. Therefore the prognostic part of the wave model covers periods from approximately 25 to 1.5 seconds. In order to include the important contribution of higher frequency waves to wave growth/dissipation processes and the output wave characteristics a parametric tail is fitted for frequencies above the spectral maximum (e.g. WAMDIG, 1988)

Wave model and source term physics configuration

The system BS-waves is based on the state-of-the-art and well-established advanced third generation spectral wave model WAM that runs successfully at many institutions worldwide. It is based on the spectral description of the wave conditions in frequency and directional space at each of the active model sea grid points of a certain model area. The energy balance equation, complemented with a suitable description of the relevant physical processes is used to follow the evolution of each wave spectral component. WAM computes the two dimensional wave variance spectrum through integration of the transport equation (1) in spherical coordinates:

$$\frac{\partial F}{\partial t}+(\cos\phi)^{-1}\frac{\partial}{\partial\phi}\left(\dot{\phi}\cos\phi F\right)+\frac{\partial}{\partial\lambda}\left(\dot{\lambda}F\right)+\sigma\frac{\partial}{\partial\sigma}\left(\dot{\sigma}\frac{F}{\sigma}\right)+\frac{\partial}{\partial\theta}\left(\dot{\theta}F\right)=S$$

with,

$F(\lambda,\phi,\sigma,\theta,t)$ wave energy density spectrum

(λ, ϕ) longitude, latitude

(σ, θ) intrinsic frequency, wave direction

$$\dot{\phi} = \left(c_g \cos\theta + u_{North}\right)/R$$
$$\dot{\lambda} = \left(c_g \sin\theta + u_{East}\right)/\left(R\cos\phi\right)$$
$$\dot{\theta} = c_g \sin\theta \tan\phi / R + \dot{\theta}_D + \dot{\theta}_C$$
$$\dot{\sigma} = \dot{\sigma}_C$$

The first term of (1) describes the local rate of change of energy density in time, the second and third ones the propagation in geographical space, the fourth one the shifting of the relative frequency due to variations in depths and currents and the last one on the left side of the equation the contribution of the depth- and current-induced refraction. The source functions on the right of the transport equation comprise the contributions of wind input (S_{in}), nonlinear interaction (S_{nl}), dissipation (S_{dis}), bottom friction (S_{bf}) and wave breaking (S_{br}) :

$S = S_{in} + S_{nl} + S_{ds} + S_{bf} + S_{br}$

A detailed description is given by the WAMDI group (1988), Komen et al. (1994), Günther et al. (1992) and Janssen (2008). The WAM Cycle 4.5.4 that is used for the Black Sea wave hindcast is an update of the former WAM Cycle 4. The basic physics and numerics are kept in that new release. The source function integration scheme made by Hersbach and Janssen (1999), and the model updates by Bidlot et al. (2007) are incorporated. The wave model performance has been discussed in Staneva at al., (2015; 2016a, b, c; Behrens, 2015).

Time dependent depth and current fields as well as assimilation of measurements into the wave fields is not used in this setup whereas wave breaking has been taken into account. The wave model WAM is not coupled to a hydrodynamic model in this application.

Forcing

The driving forces for the wave model are the U_{10} wind fields provided by the atmospheric model IFS (Integrated Forecasting System) of the ECMWF (European Centre for Medium-Range Weather Forecasts) via the CMCC server. The temporal resolution of the wind forcing is 3-h for the first 3 days of the forecast and 6-h for the rest of the forecast cycle and the hindcast. The spatial resolution of the IFS is about 14 km.

Boundary values are not required since the Black Sea is a semi enclosed area.

Initial conditions

At this release the wave model does not incorporate an observation data assimilation step when deriving its initial conditions. Instead, the initial conditions are constrained over successive cycles by including a 24 hour hindcast run of the model prior to each forecast. The role of the hindcast is to apply analysed wind fields to the wave model, so that the model is forced by the best available descriptions of atmosphere and ocean. This is an effective method of preventing any drift in wave model initial conditions, since the key response in the wave model is to the wind and the use of analysed forcing fields reduces the impact of any systematic drifts in the atmospheric model. By the same token, wave model errors are generally anticipated to be dominated by errors in the wind field after approximately 24-36 hours forecast lead time, so the benefits from using assimilation to constraining initial condition errors are unlikely to hold for forecasts beyond days one to two ahead.

Partitioning method

Included in model outputs are characteristics describing individual wave components that make up a given sea-state. For example, a sea may consist simply of a single wind-sea component for which all wave energy is affected by the forcing wind, or multiple swell components which have been remotely generated by distant storms. In WAM these components are determined using a two stage process. Individual components are derived from the two dimensional wave spectrum. This process effectively treats the wave spectrum as a topographic map from which individual peaks in wave energy can be identified in order to define the separate wave components.

The second part of the procedure follows an assumption that wind sea should be defined as only that part of the wave energy spectrum which is directly forced by the wind (this is an assumption which is most regularly used by operational wave forecasters who wish to be able to reference the evolution of wind sea directly against evolution in the local wind conditions). Using this assumption, wave spectrum bins where wave speed is slower than the (co-directed) wind speed are associated with the wind sea component. The assignment of special energy to wind sea overrides any previous assignment of wave energy to the topographic components made in the first step.

III VALIDATION FRAMEWORK

In order to evaluate and assure the quality of the BLKSEA_ANALYSIS_FORECAST_WAVES_007_003 product of the CMEMS BS-waves version V4, the system has been integrated in hindcast mode for the time period 01/12/2015 - 30/11/2017. All the satellite measurements that are available for the entire two years' time period have been used to compare the significant wave height with the corresponding wave model results. As a precondition to enable these comparisons, the satellite data has to be correlated with the wave model data in space and time. Sentinel-3a and Jason-3 need up to two minutes only to cross the Black Sea and the measurements recorded by the radar altimeter have been compared with the computed results of the nearest model output time. For each of the individual measurements with its unambiguous assignment to longitude and latitude, always the computed values of the nearest model grid point in space have been used to compare with.

Since the radar altimeter of the satellites measures wind speed and significant wave height, the only wave parameter that can be used for validation is the significant wave height (HM0).

The measured data undergoes a quality control to make sure that unrealistic values are not taken into account. Such values occur very often when the satellite passes the transition zone between land and sea at the coasts. Usually the satellites pass the Black Sea once a day, sometimes twice.

For the Black Sea, in-situ wave measurements are extreme insufficient. It has been also decided that satellite data that will be provided by Sea level IN-Situ TAC will be further used for systemic validations of the wave products.

Regarding new sources of real time data in the Black Sea to be used in the NRT validation of BS-Waves, recently measured data recorded at two moorings became available. Those are surface buoys in Burgas and Varna unfortunately directly in front of the Bulgarian Black Sea coast. First comparisons between the measured data recorded at those locations and wave model data have been done and the results are discussed in the following chapter below. The buoy stations are located at the following positions that are shown in figure 1:

Varna buoy	43.19° N	28.00° E
Burgas buoy	42.51° N	27.60° E

IV VALIDATION RESULTS

IV.1 Along track validations

The comparison between the radar altimeter measurements and the model results have been done for all satellite tracks of Sentinel-3a and Jason-3 that are available for the considered two years' period. Since the wave heights in the Black Sea are usually moderate and the differences between measured and computed data are small in those cases, several interesting situations of the period between 01/12/2015 and 30/11/2017 are discussed here. Figure 3 shows two examples for comparisons of the computed significant wave height with Jason-3 data. It includes the distribution of H_s combined with a track of the Jason-3 satellite (above) and the corresponding time series of measured and modelled wave height along the satellite track (below). On the left side, it is the descending path on 20170210 00:12:52 – 00:14:20 UTC that touches the area of maximum wave height whereas the ascending path on 20170314 09:25:06 – 09:26:46 UTC on the right side of Figure 3 directly crosses the area of maximum wave height. Both examples support a slight underestimation of the measurements by the wave model.

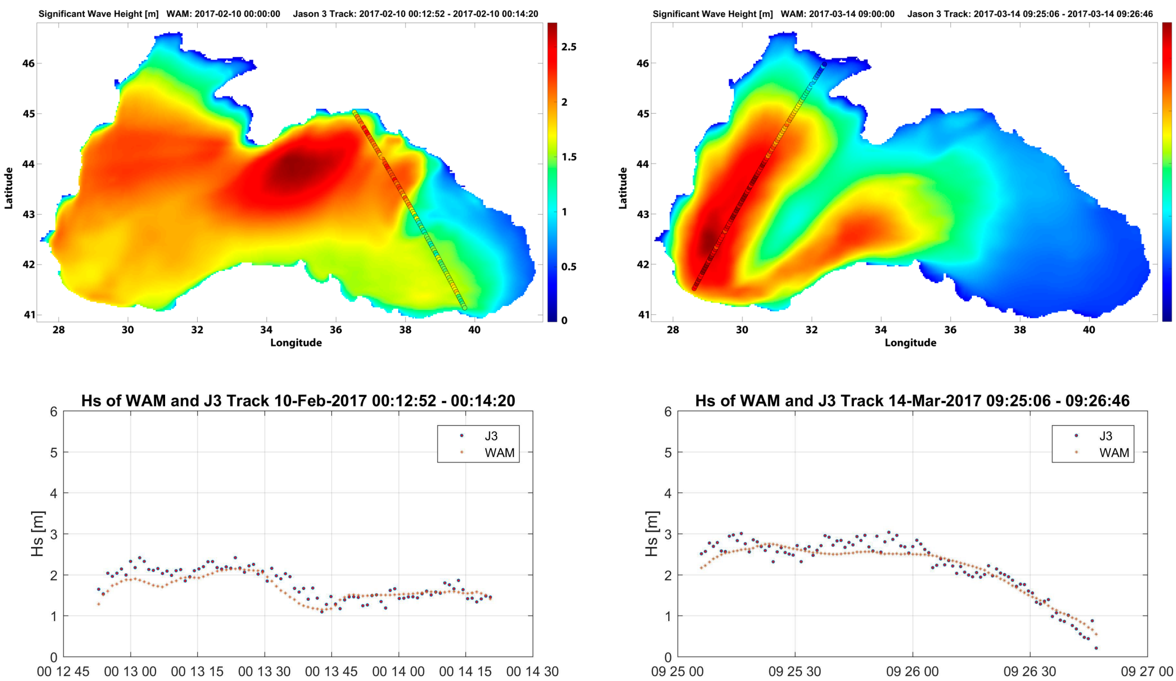

Figure 3 *: Left : distribution of H_s on 20170210 (00 UTC) and the descending Jason-3 satellite track 20170210, 00:12:52 – 00:14:20. Right : distribution of H_s on 20170314 (09 UTC) and the ascending Jason-3 satellite track 20170314, 09:25:06 -09:26:46.*

Additionally two examples for comparisons between wave model data and measured data recorded by the radar altimeter of Sentinel-3a are presented in Figure 4. The ascending satellite track on 20170216 08:25:46 – 08:27:07 UTC (left) crosses in that case an area of moderate wave height up to 2 m and the corresponding time series along the satellite path show a very good agreement between measurements and model data. The descending track on the right in Figure 4 (20170110 19:05:58 – 19:06:48 UTC) passes the area of maximum wave heights in the east with a good agreement of the wave heights up to 2.8 m as well. Finally, a slight underestimation of the measured values by the model data is detected.

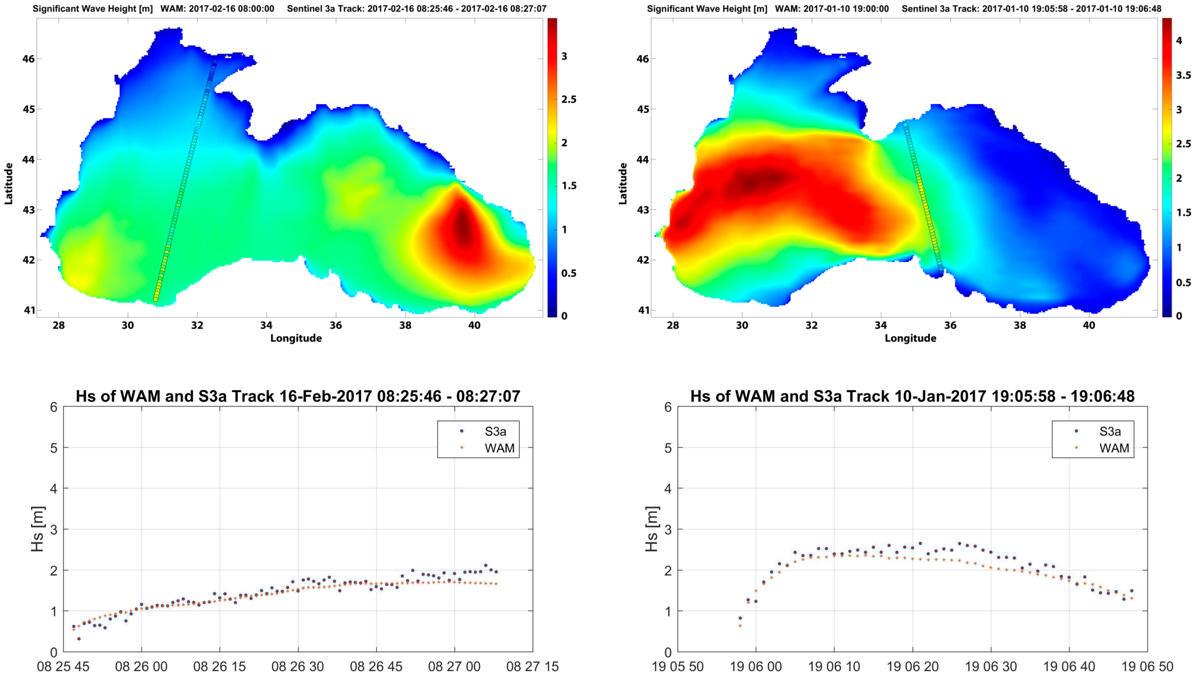

Figure 4 *: Left : distribution of H_s on 20170216 (08 UTC) and the ascending Sentinel-3a satellite track 20170216, 08:25:46 – 08:27:07. Right : distribution of H_s on 20170110 (19 UTC) and the descending Sentinel-3a satellite track 20170110, 19:05:48 -19:06:48.*

IV.2 Buoy validations

First comparisons between the measured data recorded at the locations Burags and Varna that are located near the Bulgarian coast, with wave model data have been done for the first quarter of 2016 and 2017. Figure 5 and 6 include the time series of measured and computed significant wave heights for Burgas (figure 5, 2016) and Varna (figure 6, 2016 and 2017). In general, the significant wave heights are very small during the considered time period and mainly below one meter. The three time series show a certain noise in the measurements that induces an unsatisfactory agreement between measured and modelled data. The model values follow the measured ones, but with a significant underestimation for several peaks. That is supported by the time series of the measured periods T_z in comparison with the computed T_{m2} period for the same time periods at Burgas and Varna in figure 7 and 8. Since there are no measured periods below 3 s are available in the buoy data sets, the values can be compared for periods above 3 s only. For those comparisons, the values for the computed wave periods are systematically higher as the measured ones. The small periods are very sensitive since those are computed in the high frequency range of the prognostic part of the energy balance equation.

For further use of the data obtained at Burgas and Varna, an intensive quality control of those measurements is required.

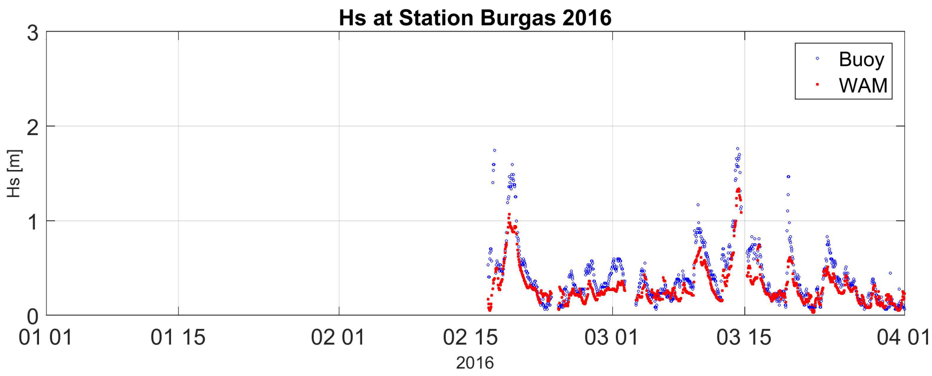

Figure 5: *Time series of measured and computed H_s at the location Burgas in 2016.*

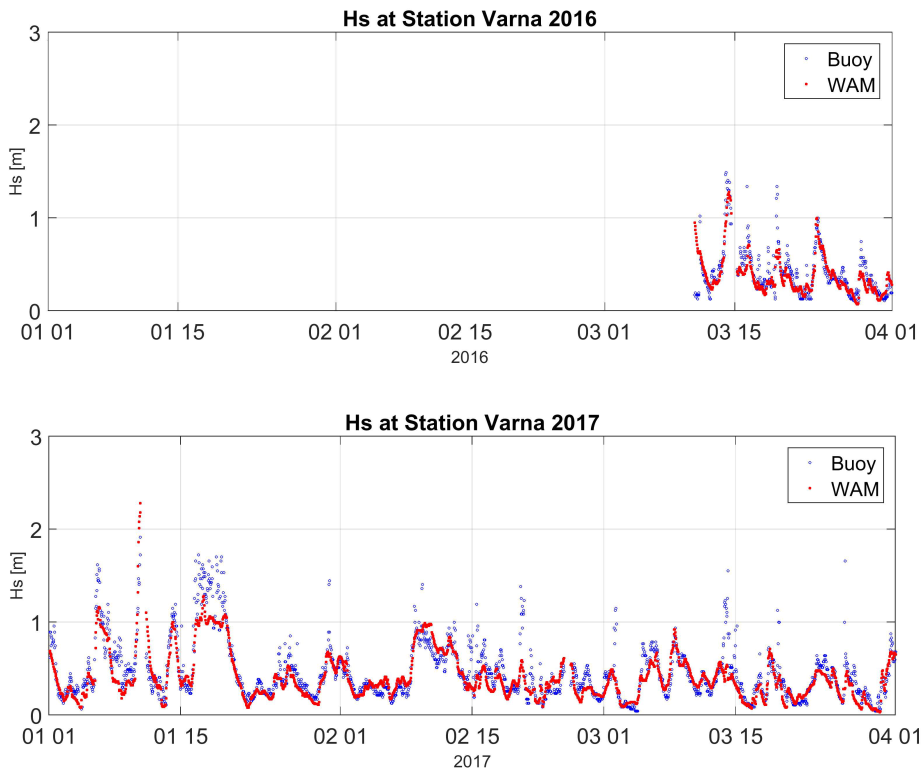

Figure 6: *Time series of measured and computed H_s at the location the Varna buoy in 2016 (above) and 2017 (below).*

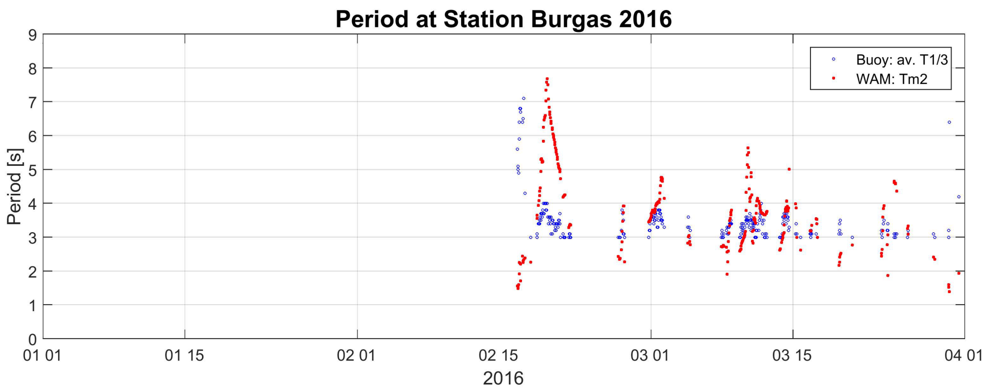

***Figure 7**: Time series of measured and computed Tz/Tm2 at the location Burgas in 2016.*

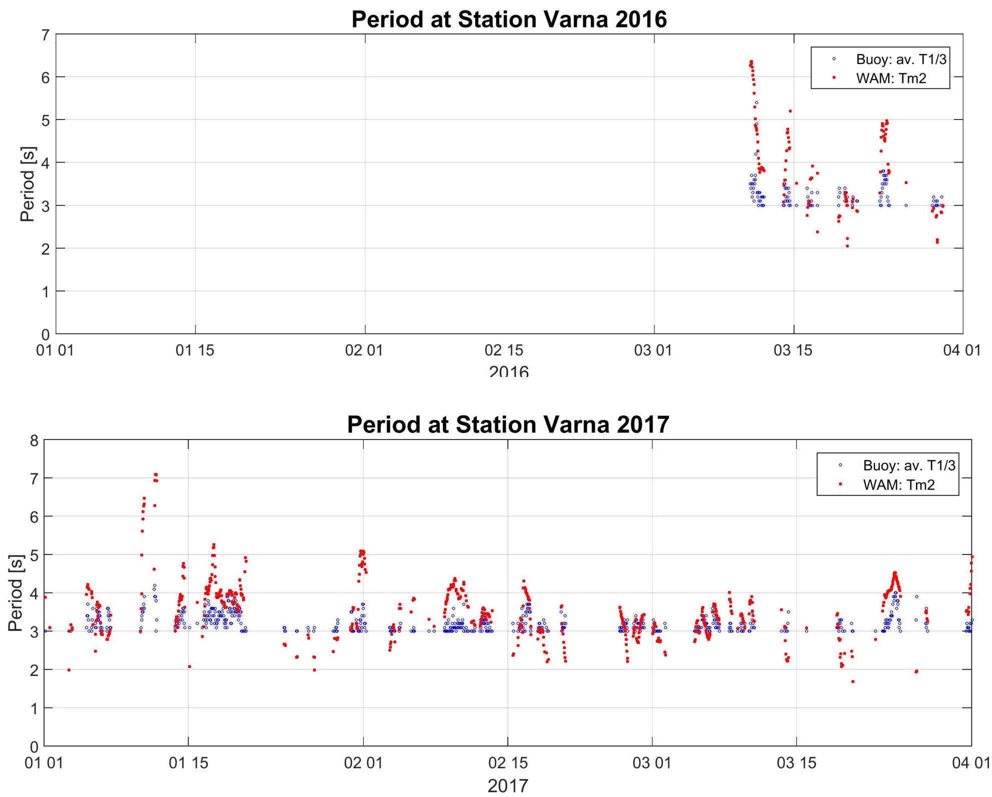

***Figure 8**: Time series of measured and computed Tz/Tm2 at the location Varna in 2016 (above) and for 2017 (below).*

IV.3 Statistics

Finally, detailed statistics following the PQWG-Waves recommendations have been calculated for all comparisons between modelled and measured data recorded by the radar altimeter of Sentinel-3a and Jason-3. For the seven quarters of the considered period (January 2016 – September 2017), the analysis for the significant wave heights is presented as a QQ-scatter plot including statistical parameters. These include the RMSD, BIAS, Scatter Index (SI), Pearson Correlation Coefficient (CORR), and best-fit Slope (SLOPE). The SI, defined here as the standard deviation of errors (model - observations) relative to the observed mean of the significant wave, being dimensionless, is more appropriate to evaluate the relative closeness of the model output to the observations at different locations compared with the RMSE, which is representative of the size of a 'typical' error. The SLOPE corresponds to a best-fit line forced through the origin (zero intercept). In addition to these core metrics, merged Density Scatter and Quantile-Quantile (QQ) are provided.

With regard to the quarterly validation procedure for the BS-waves system, the comparisons between modelled and measured satellite data have been analyzed for the four quarters of 2016 and the first three quarters of 2017. The results are shown in chapter 6. All QQ-Scatterplots on the left hand side of figures 10 and 11 include the values of the statistical parameters as well. In general, the wave model underestimates the measured data, the BIAS is negative (model – measurement).

In addition, the comparisons between the significant wave heights recorded at the two locations Burgas and Varna and the model data have been analyzed and the results are shown in Figure 9, that include the corresponding QQ-scatterplots and the values of the statistical parameters. The scatter for those comparisons is very high and supports the underestimation of the measurements by the model data. The bias computed for the examples in figure 9 varies between -7.6 and -11.6 cm.

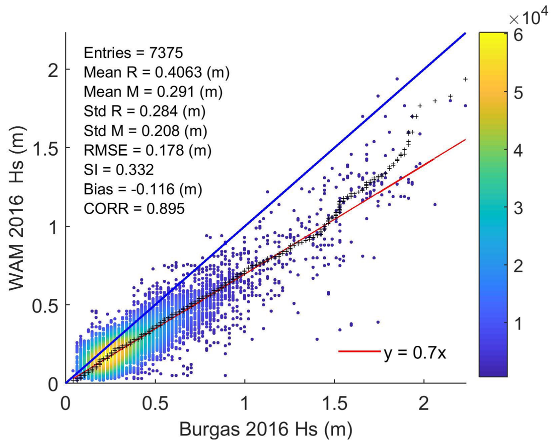

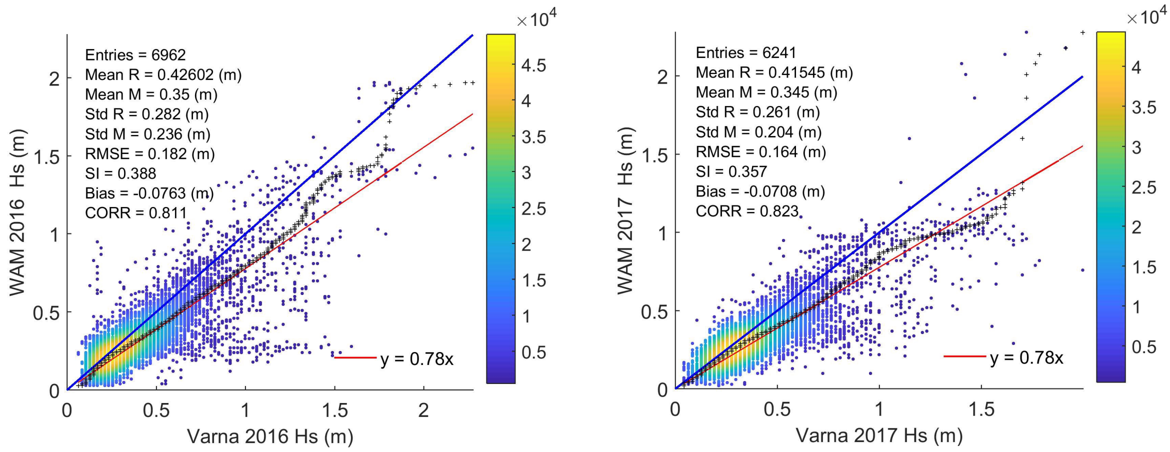

Figure 9*: QQ-Scatterplots for the comparisons between the measured wave heights recorded at the locations Burgas buoy (top 2016) and Varna buoy (bottom, left 2016 and right 2017).*

V SYSTEM'S NOTICEABLE EVENTS, OUTAGES OR CHANGES

The CMEMS BS-waves V4 system has been changed compared to the previous version CMEMS BS-waves V4. In order to reduce the underestimation of the satellite radar altimeter measurements by the wave model results, the parametrisation of the wave growth in the wind input source term has been adapted to the driving wind fields. The source term for the wind input is :

$$S_{in} = \gamma F \qquad \text{(wave growths rate * spectrum)}$$

The growth rate, normalised by the angular frequency ω, derived from a parametrization by Peter Janssen 1991 result from :

$$\frac{\gamma}{\omega} = \varepsilon \beta x^2$$

ε : air water density ratio

β : Miles parameter

$x = (\frac{u*}{c})$ max $(\cos(\theta - \varphi), 0)$

The Miles parameter β depends again on a constant that is called β_m with a value 1.2 after Peter Janssen (1991).

In the version CMEMS BS-waves V3 a value of β_m = 1.3 has been used. In contrast to that in the future version CMEMS BS-waves V4 a value of β_m = 1.5 is chosen to enable a stronger wave growth so that the significant wave heights will be higher and therefore the underestimation of the wave heights recorded by the radar altimeter of Sentinel-3a and Jason-3 will be reduced.

VI QUALITY CHANGES SINCE PREVIOUS VERSION

Due to the change in the parametrisation of the wave growth in the source term for the wind input, the quality of the wave hindcasts and forecasts is improved for the version that started in April 2018. The use of the new system CMEMS BS-waves V4 generates higher significant wave heights and reduces the underestimation of the satellite radar altimeter measurements. The statistical analysis of the comparisons between model results and measurements provides better values for the bias for the considered time period. Especially for higher waves, the agreement between model and altimeter data is improved significantly with the addition of the wave growth term. Figure 10 includes the QQ-Scatterplots for the four quarters of 2016 and the first three quarters of 2017, comparing the model results with Jason-3 data. On the left hand side, as discussed in chapter 4, the QQ-Scatterplots with the model data of the current wave model system are shown and on the right hand side, those comparing the Jason-3 data with the results obtained with the new improved wave model system. For all quarters of 2016 and 2017, a significant reduction of the negative bias could be achieved.

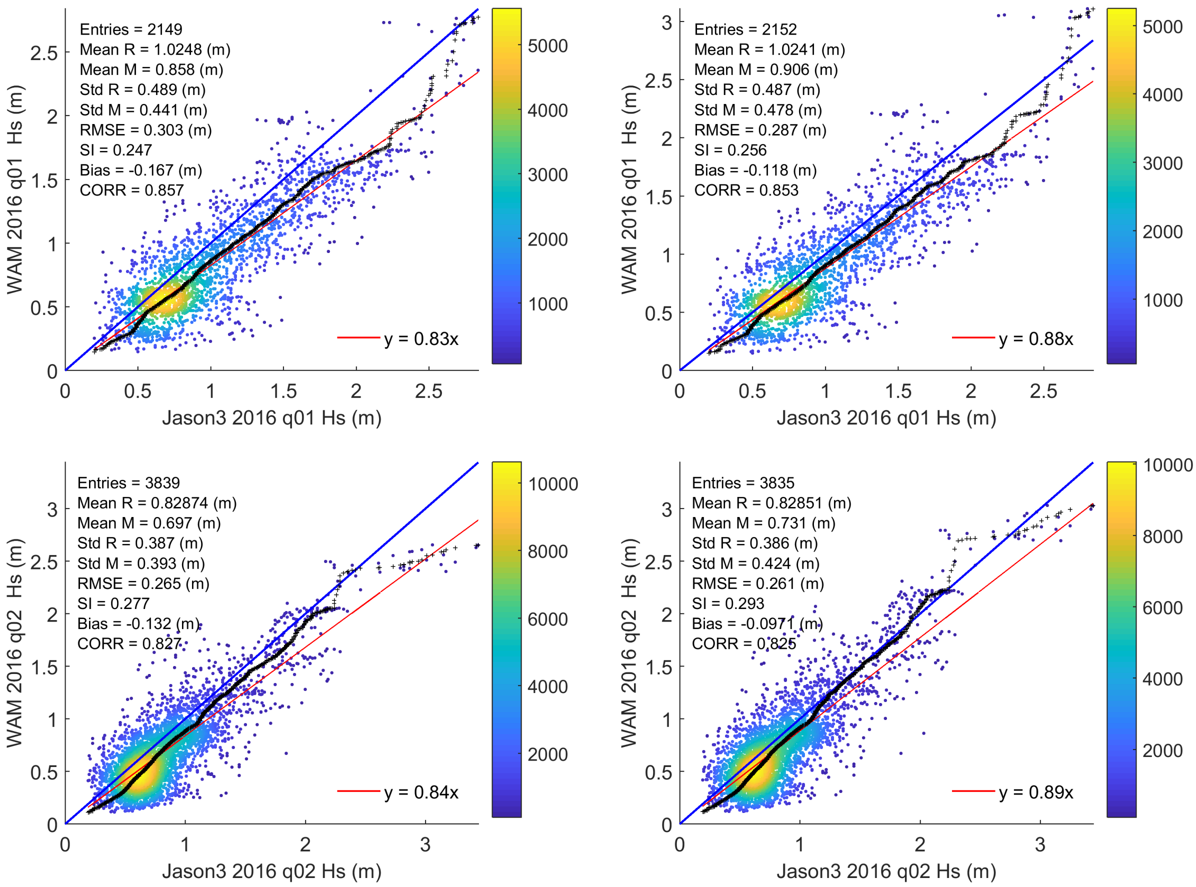

Figure 10 *: QQ-Scatterplots for the comparisons between modelled and Jason-3 data for all quarters of 2016 and the first three quarters of 2017. On the left hand side the analysis with the current wave model results, on the right hand side the model results computed with the improved wave growth (continues overleaf).*

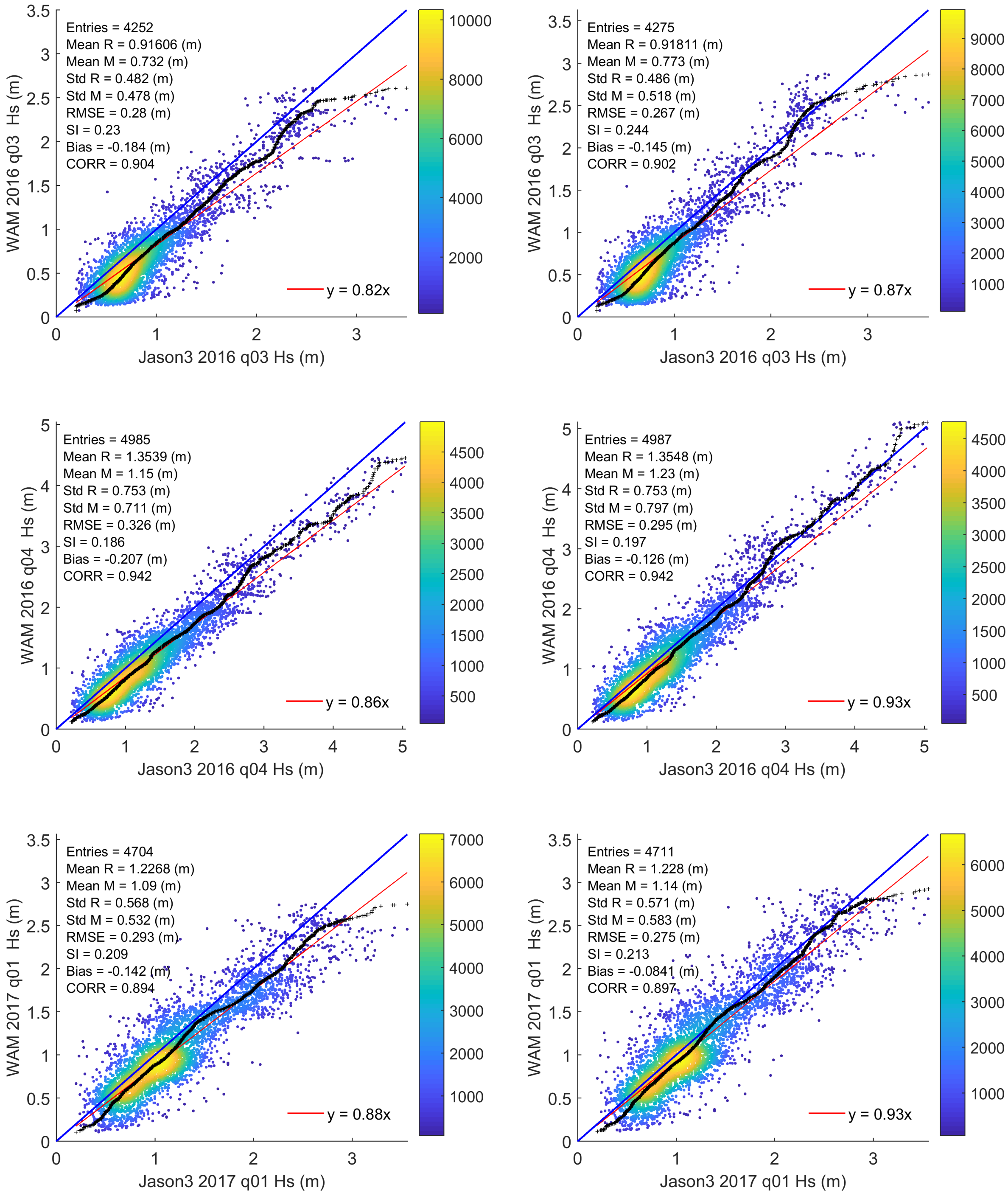

***Figure 10**: (continued) QQ-Scatterplots for the comparisons between modelled and Jason-3 data for all quarters of 2016 and the first three quarters of 2017. On the left hand side the analysis with the current wave model results, on the right hand side the model results computed with the improved wave growth.*

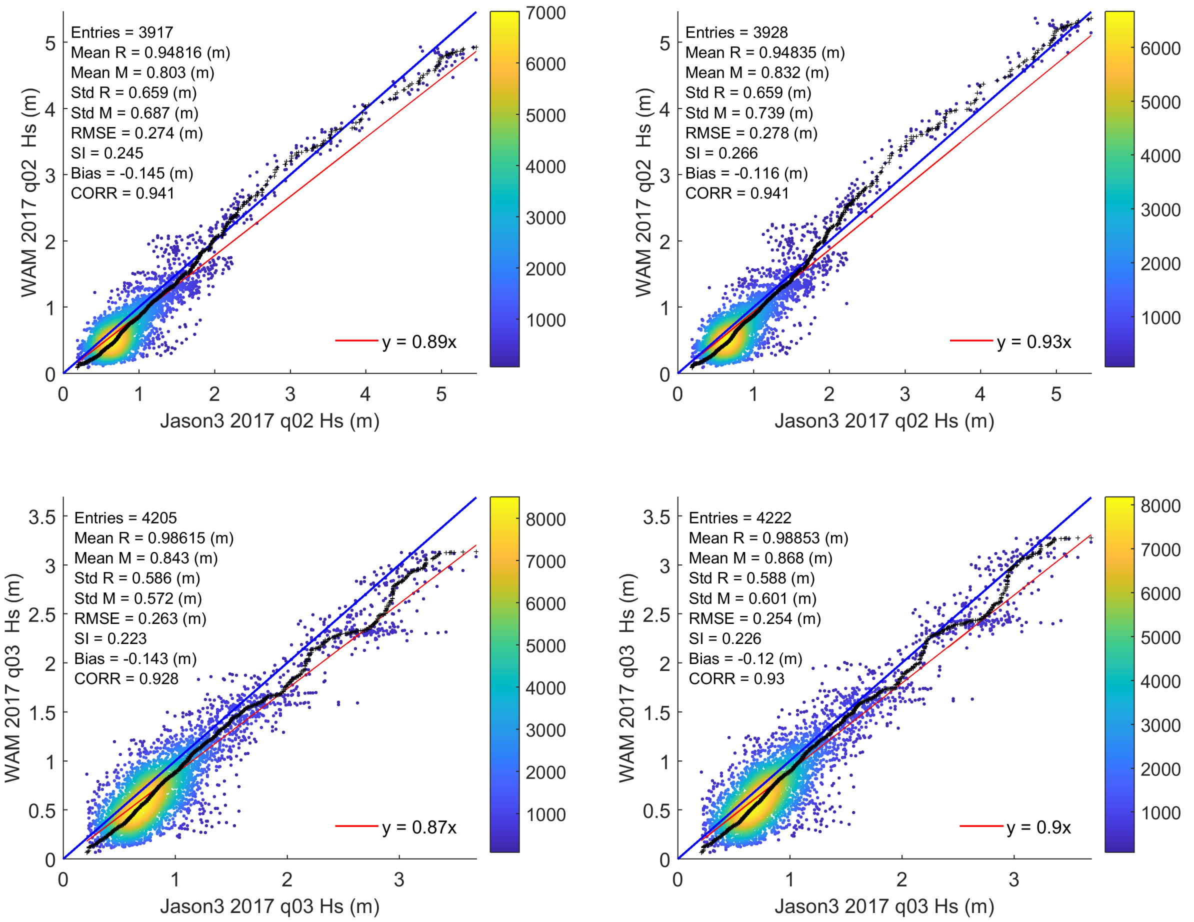

***Figure 10**: (continued) QQ-Scatterplots for the comparisons between modelled and Jason-3 data for all quarters of 2016 and the first three quarters of 2017. On the left hand side the analysis with the current wave model results, on the right hand side the model results computed with the improved wave growth.*

The same is valid for the comparisons with the current and new wave model results and the wave data recorded by the radar altimeter of the Sentinel-3a satellite. For the second quarter of 2017 no data was available and therefore only the corresponding QQ-Scatterplots for the first and the third quarter of 2017 are shown in Figure 11. The values for the bias are even higher here as those obtained in the WAM/Jason-3 comparisons. We assume that this is definitely not a problem of the wave model, but a systematic error of the measurements recorded by the radar altimeter of Sentinel-3a. Those are too high in general.

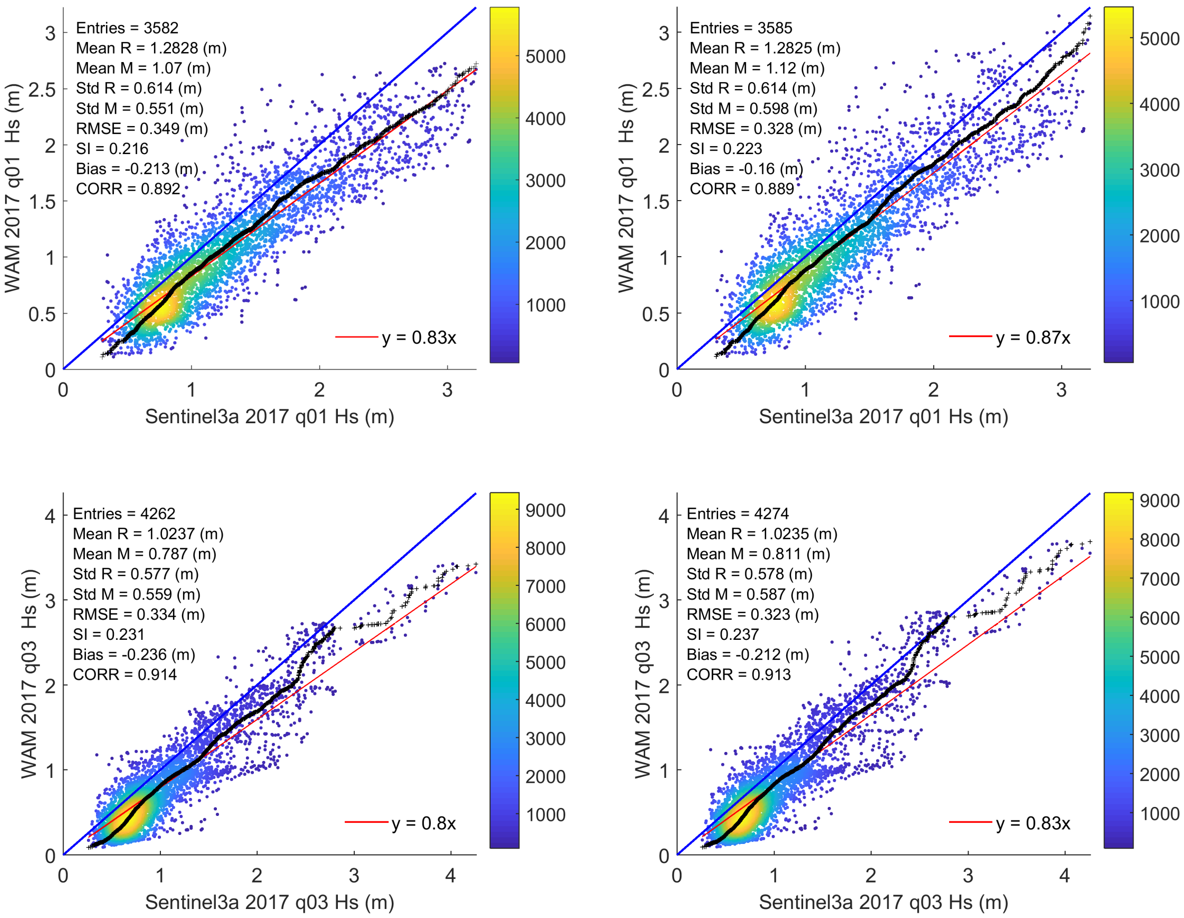

***Figure 11** : QQ-Scatterplots for the comparisons between modelled and Sentinel-3a data for the first and the third quarter of 2017. On the left hand side the analysis with the current wave model results, on the right hand side the model results computed with the improved wave growth.*

VII REFERENCES

Behrens, A., 2015 : Development of an ensemble prediction system for ocean surface waves in a coastal area. Ocean Dynamics, Volume 63, Issue 4 (2015), pp 469-486, DOI: 10.1007/s10236-015-0825-y.

Breivik, Ø, J-R Bidlot, P A Janssen (2016) A Stokes drift approximation based on the Phillips spectrum, Ocean Model, 100, 49-56, doi:10.1016/j.ocemod.2016.01.005

Breivik, Ø, P Janssen, and JR Bidlot (2014), Approximate Stokes Drift Profiles in Deep Water, J Phys Oceanogr, 44(9), 2433–2445, arXiv:1406.5039, doi:10.1175/JPO-D-14-0020.1

Dimitrova M, Kortcheva A, Galabov V (2013) Validation of the operational wave model WAVEWATCH III against altimity data from Jason-2 satellite, Bul. J. of Meteo & Hydro 18/1-2 : 4-17.

ECMWF (2015) IFS Documentation CY41R1, Book Chapter, ECMWF.

Günther H, Hasselmann S, Janssen PAEM (1992) The WAM Model Cycle 4.0. User Manual. Technical Report No. 4, Deutsches Klimarechenzentrum, Hamburg, Germany. 102 pages.

Hersbach H, Janssen PAEM (1999) Improvements of the short fetch behaviour in the WAM model. J Atmos Oceanic Tech 16: 884-892.

Janssen PAEM (1991) Quasi-linear Theory of Wind-Wave Generation Applied to Wave Forecasting. Journal of Physical Oceanography, Vol 47 No. 12.

Janssen PAEM (2008) Progress in ocean wave forecasting. J Comput Phys 227:3572-3594.

Kenyon KE (1969) Stokes Drift for Random Gravity Waves. JGR, Vol 74, No 28 : 6991-6994.

Komen GJ, Cavaleri L, Donelan M, Hasselmann K, Hasselmann S, Janssen PAEM (1994) Dynamics and Modelling of Ocean Waves, Cambridge University Press.

Kortcheva A, Dimitrova M, Galabov V (2009) A wave prediction system for real sea state forecasting in Black Sea, Bul. J. of Meteo & Hydro Vol. 1 : 1-16.

Kourafalou V., De Mey P., Staneva J., Ayoub N., Barth A., Chao Y., M Cirano M, et al., 2015. Coastal Ocean Forecasting: science foundation and user benefits, Journal of Operational Oceanography8, 147.,

WAMDI group: Hasselmann S, Hasselmann K, Bauer E, Janssen PAEM, Komen GJ, Bertotti L, Guillaume A, Cardone VC, Greenwood JA, Reistad M, Zambreski L, Ewing J (1988) The WAM model – a third generation ocean wave prediction model, J Phys Oceanogr 18: 1775-1810.

Samedo, A., Weisse, R., Behrens, A., Sterl, A., Bengtsson, L. and Günther, H. (2013): Projection of global wave climate change towards the end of the 21st century, Journal of Climate (AMS – American Meterological Society), Vol 26, pp 8269-8288

Staneva J, Alari V, Breivik O, Bidlot J-R, Mogensen K (2016) Effects of wave-induced forcing on a circulation model of the North Sea. Ocean Dynamics, DOI 10.1007/s10236-016-1009-0

Staneva J, Wahle K, Koch W, Behrens A, Fenoglio-Marc L, Stanev E (2016) Coastal flooding: impact of waves on storm surge during extremes – a case study for the German Bight, Nat. Hazards Earth Syst. Sci., 16, 2373-2389, doi:10.5194/nhess-16-2373-2016Staneva,

Staneva J., Wahle K. Günther H. and Stanev E., 2016. Coupling of wave and circulation models in coastal-ocean predicting systems: OS-2015-86, Special Issue: Operational oceanography in Europe 2014 in support of blue and green growth, 12, 3169–3197.
Staneva, J, Wahle K, Koch W, Stanev E., Fenoglio-Marc, 2016, Surge and wave predictions: Wave-current interaction during extremes in the German Bight, Ocen Science.
Staneva, J., A. Behrens and Wahle K., 2015. Wave modelling for the German Bight coastal-ocean predicting system, Journal of Physics: Conference Series, 633, pp 233-254, doi:1211, 0.1088/1742-6596/633/1/012117, ISBN: 978-3-939230-28-1
Stanev, E.V., Y. He, J. Staneva and E. Yakushev (2014) Mixing in the Black Sea detected from the temporal and spatial variability of oxygen and sulfide – Argo float observations and numerical modelling. Biogeosciences, 11, 5707–5732
Staneva, J., Behrens, A. and Groll, N. (2014): Recent Advances in Wave Modelling, Die Küste 81/2014, 233 – 254
Wahle K., Staneva J., Guenther H., 2015. Data assimilation of ocean wind waves using Neural Networks. A case study for the German Bight, Ocean Modelling, pp. 117-125
WAMDIG 1988: The WAM model - A third generation ocean wave prediction model. Journal of Physical Oceanography, 18, 1775-1810.